Anaerobes in the environment

Growth of hydrogenotrophic methanogen *Methanoculleus bourgensis* MAB1 in the presence of dunite

A. Neubeck [a,*] , N. Callac [b,1], S. Isaksson [c], A. Schnürer [c]

[a] *Department of Geological Sciences, Stockholm University, Sweden*
[b] *Ifremer, French Research Institute for Exploitation of the Sea Department of Biological Resources and Environment, France*
[c] *Department of Microbiology, Swedish University of Agricultural Sciences, Sweden*

ARTICLE INFO

ABSTRACT

This study investigated the long-term potential of low-temperature serpentinization of dunite to support the growth of the hydrogenotrophic methanogen *Methanoculleus bourgensis* strain MAB1. Incubation experiments were conducted for over 800 days, using dunite powder as the sole energy source, with and without the addition of nickel, an essential cofactor for methanogenesis. The results indicated that hydrogen released from dunite was sufficient to sustain methanogen growth, but the process was slow, with methane production beginning only after approximately 300 days. The release of toxic metals from dunite, particularly zinc, appeared to inhibit methanogen growth over time, leading to the cessation of methane production after 528 days and likely the lysing of the methanogenic cells. The study suggests that hydrogen availability, rather than nickel, is the limiting factor for methanogen growth in these conditions.

1. Introduction

In the deep subsurface, the process of serpentinization (Reaction 1) plays a key role in supporting the growth of hydrogenotrophic methanogens that use the serpentinization products as an energy source (Reaction 2). Serpentinization occurs when water reacts with ultramafic rocks such as dunite, leading to the production of hydrogen (H_2). Dunite is an ultramafic (<45 % silica) rock common in the Earth's mantle and is mainly composed of olivine ((Mg^{2+}, Fe^{2+})$_2SiO_4$) and minor amounts of other minerals common in ultramafic rocks, such as magnetite (Fe_3O_4), chromite ($FeCr_2O_4$), and pyroxene (($NaCa$)(Mg,Fe,Al)(Al,Si)$_2O_6$) and rich in Ni.

6 $(Mg,Fe)_2SiO_4$ + 7 H_2O → 3 $(Mg,Fe)_3Si_2O_5(OH)_4$ + Fe_3O_4 + H_2 (Reaction 1)

CO_2 +4H_2 →CH_4 +2H_2O (Reaction 2)
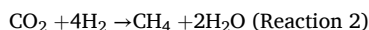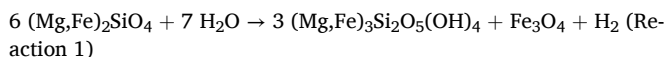
Due to the simplicity of the energy-generating CO_2-H_2 reaction (Reaction 2) of hydrogenotrophic methanogens, it is considered an ancient metabolic pathway [1] likely evolving in marine hydrothermal vent systems where CO_2, H_2, and acetate are abundant [2]. However, the

way serpentinization supports methanogen activity is deeply influenced by temperature variations and the migration of gases like H_2 and CO_2 through the subsurface. Serpentinization typically takes place at elevated temperatures of around 200 °C–300 °C, deep in the Earth's crust [3]. At these high temperatures, the reaction between water and the mineral olivine found in dunite generates serpentine minerals, magnetite, and $H_{2(gas)}$. While this H_2 is vital for methanogen survival, these microorganisms cannot thrive in such extreme heat, as they generally grow best in much cooler environments, between 20 °C and 60 °C [4]. For this reason, the H_2 produced at depth migrate to cooler regions and indirectly fuel methanogenic growth in close vicinity to the serpentinization. Direct H_2 fueling of methanogens in cooler serpentinization regions is less studied [5] partly due to the slow rate of dunite alteration at low temperatures and partly due to the lack of knowledge on methanogens-mineral interactions.

Methanogens play a crucial role in the biogeochemical cycling of essential elements [6]. Recent studies have shown that methanogens are capable of extracting Fe and S from iron-rich minerals like pyrite (FeS_2) through reductive dissolution [7]. Pyrite, being conductive, serves as an energy transport bridge for methanogens. Another conductive mineral, magnetite (Fe_3O_4), which is commonly formed as a product of

* Corresponding author.
E-mail address: anna.neubeck@geo.uu.se (A. Neubeck).
[1] Present address: Ifremer, IRD, Université de la Nouvelle-Calédonie, Université de La Réunion, CNRS, UMR 9220 ENTROPIE, 98800 Nouméa, New Caledonia.

serpentinization (Reaction 1), may also facilitate energy transport for methanogens [8]. This means that methanogens can potentially use conducting minerals as electron donors to reduce CO_2 to CH_4, bypassing the need for H_2 in this process [9]. Thus, minerals in the deep subsurface with a limited supply of energy, may be used as direct electron transferrer maybe even when the amount of H_2 is limited, such in a low temperature ultramafic system, where the serpentinization reaction may be too slow for an efficient abiotic formation of H_2. Utilization of electrons or H_2 (through oxidation) by methanogens is mainly performed by enzymes with nickel (Ni) and iron (Fe) as their active site metal center (so-called [NiFe]-hydrogenases) highlighting the need for Fe and Ni [6,10,11]. Methanogens require Fe and Ni for their survival, but the requirement varies depending on genus [12,13]. They contain three of the seven known Ni-containing enzymes [14] 1) CO dehydrogenase/acetyl-CoA synthase (CODH/ACS), an enzyme for carbon fixation, 2) hydrogenase, an enzyme for oxidation of H_2, and 3) cofactor F_{430} in the enzyme methyl-coenzyme M reductase (MCR), which is involved in the formation of CH_4 in all methanogens [15]. Other than H_2 and CO_2, methanogens have a high demand for metals such as Fe and Ni, due to the diverse abundance of metalloproteins involved in the formation of CH_4 from H_2 and CO_2.

The primary objective of this study to provide insights into the viability of methanogenic activity in ultramafic rock environments and the geochemical factors that limit or promote CH_4 production in such settings. More specifically the study aims to investigate the long-term potential of low-temperature serpentinization of dunite to support the growth and survival of hydrogenotrophic methanogens. Additionally, the study seeks to evaluate the influence of nickel supplementation, an essential cofactor for methanogenesis, on and CH_4 production rates. For the study the *Methanoculleus* strain MAB1, was selected. This methanogens has been shown to be able to grow at very low H_2 concentrations [12] and *Methanoculleus* have been identified in various deep subsurface environments [16,17].

2. Materials and methods

2.1. Methanogen

The hydrogenotrophic methanogen *Methanoculleus bourgensis* strain MAB1 (hereafter 'MAB1') was used for the growth experiments. This organism is an hydrogenotrophic methanogen growing with H_2 and CO_2 or formate and using small levels of acetate as extra carbon source [18]. MAB1, in similar to other species of genus *Methanoculleus*, does not use acetate as an energy source for CH_4 production [18]. This methanogen was chosen for the experiment due to its ability to grow at very low pH_2 [12]. MAB1 was provided by the Department of Molecular Sciences, Swedish University of Agricultural Sciences, Uppsala.

2.2. Preparation of cultivation bottles

Prior to the experiments, all borosilicate glass bottles, black butyl-rubber stoppers (Gotlands gummifabrik), and plastic disposables used in the experiment were acid-washed to remove metal contaminants by soaking in 20 % HCl for 24 h, followed by soaking in pure Milli-Q water (resistivity: 18.2 M Ω cm^{-1}) for another 24 h. The bottles were then covered with perforated plastic film and dried overnight at 70 °C before use. All acid washed disposables and rubber septa were also dried overnight at 70 °C before use.

2.3. Preparation of dunite

Natural forsteritic dunite (forsterite 92 (Fo92) artificially crushed dunite) was obtained from North Cape Minerals in Åheim, Norway. Contaminants, such as steel fragments (from crushing the dunite) and magnetic accessory minerals that could affect the results of the experiments because of their strong reducing capacity, were removed using a

Frantz magnetic separator. The dunite was cleaned with water (pure Milli-Q water) until all fine particles (<63 μm) and dust were removed ($\sim$15 times). Thereafter, the dunite was cleaned with acetone (Merck, SupraSolv) in an ultrasonic bath, 3 times for 15 min and dried (100 °C) overnight. When dry, dunite was hand-milled in an ethanol-cleaned agate mortar and pestle to a fine powder (grain size <63 μm). Approximately 1 g of dunite powder was added to acid-washed cultivation bottles. The bottles were closed with acid washes butyl-rubber stoppers and aluminum caps and then dry-sterilized (125 °C, 8h) to remove possible bacterial contaminants.

2.4. Preparation of anaerobic medium

For cultivation of the methanogen a bicarbonate-buffered basal medium (BM) was prepared as previously described [12,19]. To minimize possible uncontrolled sources of carbon and Ni, yeast extract and resazurin was omitted from the growth medium. In short, phosphate buffer and water were mixed and boiled for approx. 20 min and thereafter cooled under flushing with N_2 to reduce levels of oxygen. After cooling, the medium was supplemented with sodium acetate (0.42 g L^{-1}) to support biosynthesis of the methanogen. Subsequently, the medium (18 ml) was distributed into serum bottles (118) under flushing with N_2. The bottles were closed with butyl rubber stoppers and aluminum rings and the gas phase in the bottles were exchanged three times and finally pressurized to 0.2 atm with N_2 and autoclaved for 20 min at 121 °C. After cooling, the medium in each bottle were supplemented with C1 (1 ml), containing vitamins, salts, and trace metals and C2 (1 ml), containing bicarbonate and reducing agents. The solutions C1 and C2 were prepared as described before [12] and sterile-filtered (0.2 μm) into closed autoclaved vials filled with N_2. The final pH of the final medium was 7.3.

For incubations without Ni, C1 solution was also prepared without addition of this trace metal. However, the Milli-Q water used for preparation of the medium contained some Ni and, consequently, traces of Ni were present at the onset of the experiments. The average concentration of Ni in the final "Ni-free" medium was approximately 2.5 μg L^{-1}, analyzed using an Inductively Coupled Plasma Atomic Emission Spectroscopy (ICP-AES) instrument, calibrated using standard solutions (Multi-element standard solutions, LGC-Promochem, chromatography grade) and a blank (Milli-Q water). The analytical error was approximately 4 %.

2.5. Experiment design

The experiment was set up according to Table 1. In short three replicates (A, B, C) were prepared for each set of biotic and abiotic incubation. For one set up (MAB1-Ni + Du) in total 6 replicates were prepared. For the biotic set up, actively growing MAB1 (2 ml) was added to the cultivation medium (20 ml), with and without Ni and dunite, using a sterile syringe. Before inoculation the methanogen was pre-grown in the bicarbonate-buffered basal medium (BM) prepared as

Table 1
Experiment set-up, where Ni = nickel, Du = dunite, and A, B, C are replicate incubation bottles.

Biotic	Components	Notes
1 (A, B, C)	MAB1+Ni + Du	
2, 6 (A, B, C, A, B, C)	MAB1-Ni + Du	
4 (A, B, C)	MAB1+Ni-Du	
8 (A, B, C)	MAB1-Ni-Du	
Abiotic controls	**Setup**	
3 (A, B, C)	Ni + Du	
5 (A, B, C)	Ni	
9 (A, B, C)	+Du	
10 (A, B, C)		Only growth medium without Ni

previously described, using H_2/CO_2 (1 atm, 80:20) and sodium acetate (0.42 g/L) as energy and carbon source, respectively. Yeast extract and resazurin was excluded from the medium to minimize the level of non-defined carbon sources. The pre-cultivation was made in 430 ml medium in a 1L serum bottle. This means that all the inoculations in the experimental set up was made using the same batch of methanogenic culture. For incubation with dunite, 18 ml sterile and reduced medium was transferred with a syringe to the mineral supplemented bottles. The abiotic controls were prepared in the same way with the difference that no methanogen was added. The dissolved element concentrations at the start and end of the experiment were measured in 5 mL aliquots of liquid extracted from the bottles using a sterile needle. An estimation of redox conditions was evaluated at the end of the experiment by addition of the redox indicator resazurin, which turns pink at -60 mV. The experiment was run for more than 800 days and at the end (day 829) methanogenic survival and activity was evaluated by addition of external H_2-CO_2 (80:20) to an overpressure of 1 atm followed by analysis of CH_4 and H_2.

2.6. Microscopic analyses (SEM)

A subsets of cell samples from the cultivation bottles were optically investigated using a Scanning Electron Microscope (SEM) coupled to an energy dispersive spectrometer (EDS) on an FEI QUANTA FEG 650 (Oxford Instruments, UK). The instrument was calibrated using a cobalt standard. Peak and element analyses were performed using INCA Suite 4.11 software. For the analysis by EDS, an Oxford T-Max 80 detector was used. The samples were first fixed in 2 % glutaraldehyde in 0.1 M sodium phosphate (pH 7.4) and filtered through a 1000 kDa PES membrane (Pall Corporation). The filtered membrane was subjected to stepwise ethanol dehydration, followed by critical point drying using an EM CPD030 (Leica Microsystems). The dried membrane was finally sputter-coated using a Q150T ES (Quorum Technologies) and SEM images were acquired using a Zeiss Ultra 55 FE-SEM microscope (Zeiss) with an in-lens detector at 3 kV. The samples were gold-coated and kept under low-vacuum conditions and a low acceleration voltage of 20 or 15 kV, to minimize surface charging effects.

2.7. Analytical methods

Before and after the experiments, subsets of powdered dunite samples were investigated using a Powder X-Ray Diffractometer Panalytical X'Pert alpha1 at the Department of Material and Environmental Chemistry at Stockholm University, with the purpose of identifying presence of serpentine minerals. The samples (powdered) were analyzed by placing the sample on a zero-background silicon wafer. The software HighScore Plus was used to identify peaks and minerals. The metal concentrations in the cultivation bottles were analyzed by withdrawing 10 mL of fluid from each bottle for analyses using ICP-AES analysis. Before analysis the samples were acidified with nitric acid (65 %, p.a, Merck). Multi-element calibration standards were prepared by dilution of appropriate element stock solutions (Teknolab A/S, Drobak, Norway; Referensmaterial AB, Ulricehamn, Sweden and BDH Chemicals Ltd., Pool, England) in 80 mM HNO_3. A Spectro Ciros CCD ICP-AES (Spectro, Germany) was used for the determination of element concentration. A standard solution and blank solution were regularly measured to check for drift and contamination.

Acetate concentration was quantified after termination of the experiments using High Performance Liquid Chromatograph (HPLC) analyses. The HPLC (Aligent 1100) was equipped with an ion exchange column (Rezex-ROA-Organic Acid H^+) and a refractive index detector. The column was operated at 60 °C and 5 mM H_2SO_4 was used as the eluent at a flow rate of 0.6 mL min^{-1} [13].

Hydrogen (H_2) and carbon monoxide (CO) partial pressure (pH_2, pCO) were analyzed by PP1 (Peak Performer 1, reduced gas analyzer) by direct injection of 1 mL withdrawn from the headspace gas. Methane (CH_4) samples (2 mL) were withdrawn at the same time, injected into

glass vials, and stored at $+2$ °C until analysis (within a maximum of 5 days) by gas chromatography (GC) (PerkinElmer Ariel, Clarus 500 Gas Chromatograph equipped with a TurboMatrix 110 Headspace sampler) [19].

2.8. DNA extraction and microbial analysis

Total DNA was extracted from culture liquid withdrawn at the endpoint of the experiment from all experimental bottles, including both inoculated cultures and controls. A total of 4 mL of liquid was collected using a syringe and used for triplicate extractions with the DNeasy Blood and Tissue Kit (QIAGEN), following the manufacturer's instructions.

Methanogenic abundance was determined by quantitative real-time PCR (qPCR) using the CFX Connect™ Real-Time System (Bio-Rad). Each PCR reaction contained 10 μL of $2 \times$ iQ SYBR Green Supermix (Bio-Rad), 5 μL of nuclease-free water, 3 μL of template DNA ($\sim$7 ng μL^{-1}), and 1 μL of each methanogen-specific primer Met630F/Met803R (10 pmol μL^{-1}) [20]. The qPCR program consisted of an initial denaturation at 95 °C for 7 min, followed by 40 cycles of 95 °C for 40 s, 60 °C for 60 s, and 72 °C for 40 s. A melt curve analysis (55–95 °C, $\Delta T = 0.1$ °C s^{-1}) was performed to assess specificity.

A standard curve was constructed according to Ref. [20], using the amplicon obtained from MAB1 genomic DNA with the primers and PCR conditions described above (30 cycles). The qPCR achieved an efficiency of 96.5 % with a linear correlation coefficient (r^2) of 0.984.

To identify possible contaminating bacterial components in the samples, PCR was performed targeting the bacterial 16S rRNA gene using the primers E8F (5'-AGAGTTTGATCATGGTCAG-3') and U907R (5'-CCGTCAATTCMTTTGAGTTT-3') [21]. The analysis was conducted on the same DNA samples used for the qPCR analysis of methanogens. PCR products were verified by gel electrophoresis, purified, and sequenced at Macrogen (Korea). The obtained sequences were analyzed using the BLAST nucleotide search program through the National Center for Biotechnology Information (NCBI, http://www.ncbi.nlm.nih.gov/BLAST). In total, five samples (4A, 4B, 4C, 8A, and 8C) yielded a PCR signal. Forward and reverse sequences were aligned to generate a consensus sequence (1332–1441 bp). The aligned sequences were taxonomically identified by BLAST using the NCBInr database, showing 96.8–98.1 % similarity with *Limnochorda pilosa* (strain HC 45, whole genome, accession number AP014924.1) [22]. Sequences are deposited in the GenBank nucleotide sequence database under accession numbers MN816749–MN816753.

2.9. Statistical analyses

One-way multivariate analysis of variance (MANOVA), using Wilks' lambda test, was performed on the entire experiment (from beginning to the end), to test the similarity between replicate experiments and determine whether biotic and abiotic pairs incubated under the same conditions were similar or different in terms of CH_4 production and H_2 and CO concentration through the experiment. Values of $P < 0.05$ were considered statistically significant.

The biotic and abiotic pairs tested were: inoculated and non-inoculated experiment with Ni and with dunite (batch 1 against 3); inoculated and non-inoculated experiment with Ni and without dunite (batch 4 against 5); inoculated and non-inoculated experiment without Ni and with dunite (batch $2 + 6$ against 9); and inoculated and non-inoculated experiment without Ni and without dunite (batch 8 against 10). Principal component analysis (PCA) was conducted to examine correlations between CH_4, H_2, and CO concentration in the presence or absence of Ni and dunite in both biotic and abiotic experiments, for the whole duration of the experiment.

To test similarity in CH_4 production between the different biotic incubation conditions (with or without Ni and dunite), we performed one-way ANOVA using Tukey's test. Conditions tested were: presence of dunite with or without Ni (batch 1 against batch $2 + 6$); absence of

dunite with or without Ni (batch 4 against 8); presence of Ni with or without dunite (batch 1 against 4); and absence of Ni with or without dunite (batch 2 + 6 against 8). Values of $P < 0.05$ were considered statistically significant. In addition, to examine the correlation between CH_4 production and presence or absence of Ni and dunite in the biotic experiments, PCA analyses was conducted. All statistical analyses were performed using XLSTAT (Addinsoft), a statistics tool appended to Microsoft Excel.

3. Results

3.1. Hydrogen and CO consumption and production

The initial H_2 level at the beginning of the experiment was approximately 9 mmol L^{-1} in all samples inoculated with the methanogen and around 2 mmol L^{-1} in non-inoculated controls. The starting level of H_2 was higher in the inoculated samples as small amounts of H_2 was included with the transferred portion of the pre-grown methanogenic culture. Thereafter, a clear decrease in the amount of H_2 in the gas phase was seen in the biotic samples until day 528–600, reaching a level of approximately 0.5–5 mmol L^{-1}, corresponding to ca 0.1–1.5 Pa (Fig. 1, Table 2).

After 600 days of incubation, the concentration of H_2 in the inoculated bottles with dunite started to increase steadily until day 829 and at that time reaching 13.3 ± 6.9 mmol L^{-1}. For the rest of the bottles the average amount of H_2 over the whole experimental period was significantly lower (<1.9 mmol L^{-1}) as compare to the bottles with dunite.

A clear statistically significant difference in CO levels was observed between abiotic controls and biotic samples, with the inoculated samples generally having a lower concentration of CO (Fig. 2). Moreover, the biotic experiments with added Ni had a higher initial CO content than the experiments without added Ni. At termination, the biotic experiments with added dunite had a higher amount of CO than the experiments without dunite. In the abiotic control experiments the opposite trend was observed, with the experiments with added dunite having a lower amount of CO than the experiments without added dunite.

3.2. Methane production

Accumulation of CH_4 proceeded slowly in all bottles inoculated with MAB1 during the first ~300 days and reached a cumulative level of approx. 3.1 ± 1.6 µmol L^{-1} after 305 days (Fig. 3). In the abiotic control

the levels were approx. 1.6 ± 0.6 µmol L^{-1} after 305 days. Thereafter, CH_4 production in the inoculated bottles increased rapidly to a maximum average level between 1.5 ± 0.1–4.2 ± 0.3 mmol L^{-1} after approx. 528 days, after which production levelled off (Fig. 3). The final CH_4 level differed slightly in the bottles and levels decreased in the order MAB1-Ni + du > MAB1+Ni + du > MAB1+Ni-du > MAB1-Ni-du. The abiotic controls, independent of presence of Ni or dunite or not, had a very low CH_4 level, ranging from approximately 0–0.04 mmol L^{-1} (accumulated values) after day 305. At the end of the experimental period (day 950 H_2 was added (H_2-CO_2 (80:20) to an overpressure of 1 atm) to investigate methanogenic activity. This resulted in a significant increase of methane in the inoculated bottles without dunite, reaching 4.6 ± 0.5 CH_4 mmol/L (data not shown). In contrast, no response was seen in the dunite supplemented bottles with MAB1 or for the abiotic controls.

3.3. Major element concentration and acetate measurements

The concentrations of Si, Mg, Ni, Fe, and Zn in all bottles after termination of the experiments revealed comparably higher concentrations of all elements in the dunite supplemented bottles compared to non-supplemented bottles (Table 3). The inoculated bottles supplemented with dunite had a comparably higher concentrations of Si and Zn. In the bottles without dunite, Ni, Fe and Zn were below detection limit (Table 3). For acetate, added as carbon source for the methanogen, concentration declined to almost zero in the inoculated samples without added dunite, while the concentration in the non-inoculated bottles was similar to initial levels (0.3 g/L) (Table 3).

3.4. Microscopic analyses

Microscopical evaluation of the dunite grain surface at the end of the experiment using optical microscopy revealed as expected presence of an irregular cocci, the morphology of *Methanoculleus*, but also as well some filamentous cells, indicating bacterial contamination (Fig. 4a). In addition, a large amount of very small (<0.1 µm) sphere shape structures were observed (Fig. 4b). Precipitates (secondary minerals and/or evaporites) were also detected through visual and analytical measurements using SEM (Fig. 4c).

3.5. Microbial analyses

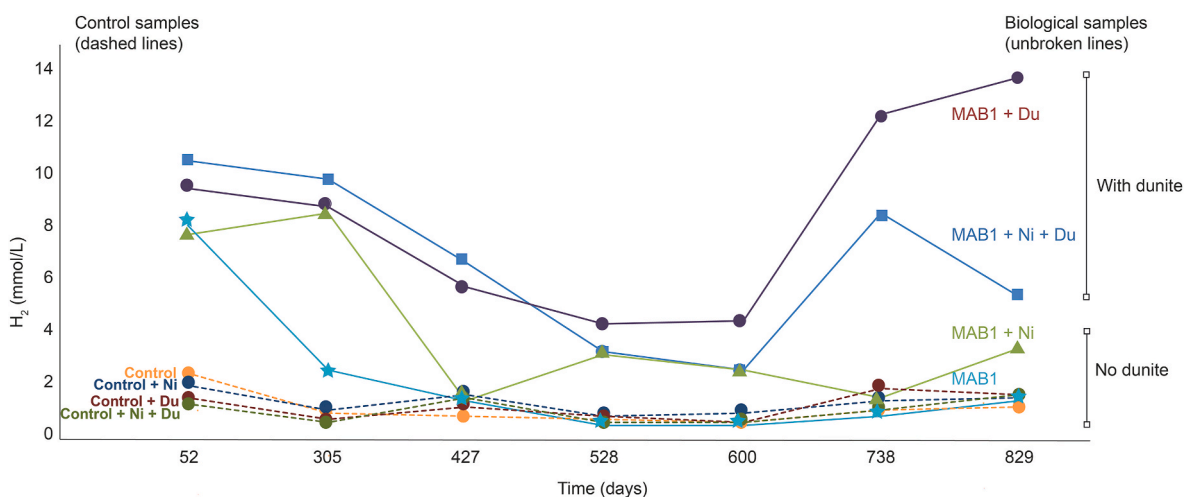Samples were taken from all bottles (except 2a which was used for

Fig. 1. Average (of three replicates) H_2 level (mmol L^{-1}) in the inoculated bottles and abiotic controls. Error bars values presented in Table 2, below. Open symbols represent experiments with added dunite, filled symbols without added dunite. Dashed lines represent control samples.

Table 2
Mean amount of H_2 (mmol L^{-1}) and partial pressure of H_2 (pH_2 in bold, calculated from the average H_2 value) in the experimental bottles. GM = non inoculated growth medium.

Experiment setup	Time (days)													
	52		305		427		528		600		738		829	
MAB1+Ni + Du	10.3 ± 0.9	**3**	9.6 ± 0.8	**2.8**	6.5 ± 1.5	**1.9**	3.2 ± 1.7	**0.9**	2.5 ± 1.7	**0.6**	8.3 ± 6.4	**2.1**	5.3 ± 3.3	**1.5**
MAB1+Du	9.2 ± 0.5	**2.8**	8.5 ± 0.8	**2.6**	5.6 ± 2.8	**1.7**	4.2 ± 0.3	**1.2**	4.3 ± 2.3	**1.1**	11.9 ± 3.9	**3.1**	13.3 ± 6.9	**3.7**
MAB1+Ni	7.5 ± 0.3	**1.9**	8.3 ± 2.3	**2.1**	1.4 ± 0.7	**0.4**	3.1 ± 2.2	**0.8**	2.5 ± 3.7	**0.6**	1.5 ± 1.6	**0.3**	3.3 ± 2.7	**1**
MAB1	7.9 ± 0.7	**2**	2.6 ± 1.2	**0.7**	1.4 ± 1.0	**0.3**	0.5 ± 0.3	**0.1**	0.5 ± 0.4	**0.1**	0.8 ± 0.7	**0.2**	1.4 ± 1.0	**0.3**
Control (+Ni + Du)	2.4 ± 2.2	**0.4**	0.9 ± 2.5	**0.2**	0.8 ± 2.3	**0.4**	0.7 ± 1.4	**0.2**	0.6 ± 2.0	**0.2**	1.0 ± 4.6	**0.3**	1.1 ± 4.5	**0.5**
Control (+Ni)	2.0 ± 1.0	**0.5**	1.1 ± 0.4	**0.3**	1.7 ± 0.6	**0.4**	0.9 ± 0.3	**0.2**	1.0 ± 0.1	**0.2**	1.4 ± 0.3	**0.3**	1.5 ± 0.2	**0.5**
Control (+Du)	1.5 ± 0.3	**0.4**	0.7 ± 0.1	**0.2**	1.2 ± 0.7	**0.4**	0.8 ± 0.1	**0.2**	0.6 ± 0.2	**0.2**	1.9 ± 0.8	**0.5**	1.6 ± 0.4	**0.5**
Control	1.3 ± 0.6	**0.6**	0.6 ± 0.3	**0.2**	1.5 ± 0.8	**0.2**	0.6 ± 0.4	**0.2**	0.6 ± 0.3	**0.1**	1.1 ± 0.6	**0.2**	1.6 ± 0.9	**0.4**
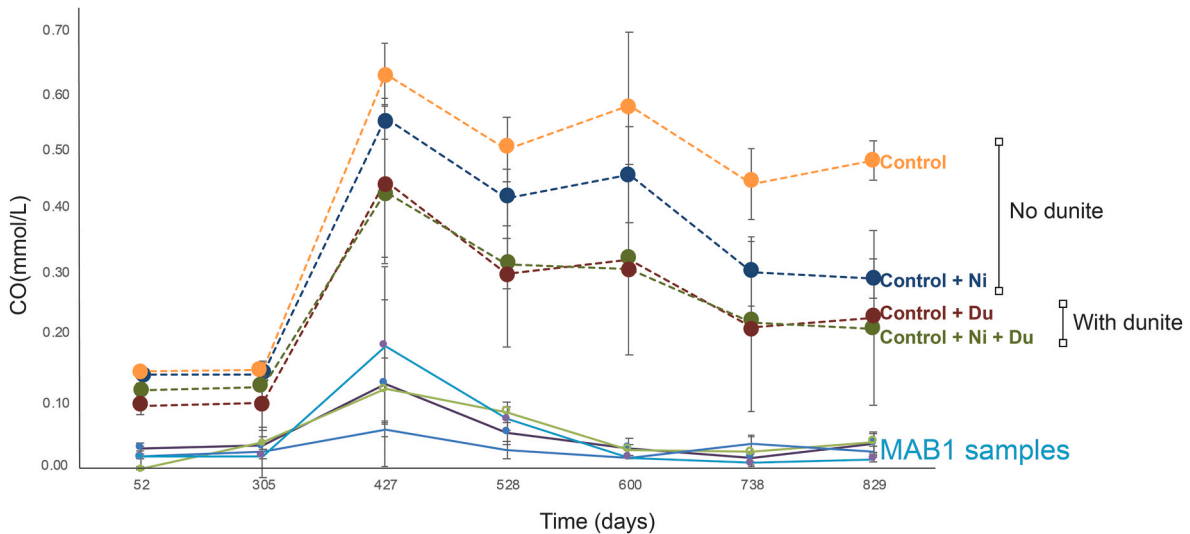
Fig. 2. Average (of three replicates) levels of carbon monoxide (CO, mmol L^{-1}) in the inoculated bottles and abiotic controls. For treatment abbreviations, see Table 1. Open symbols represent experiments with added dunite, filled symbols without added dunite. Dashed lines represent control samples.
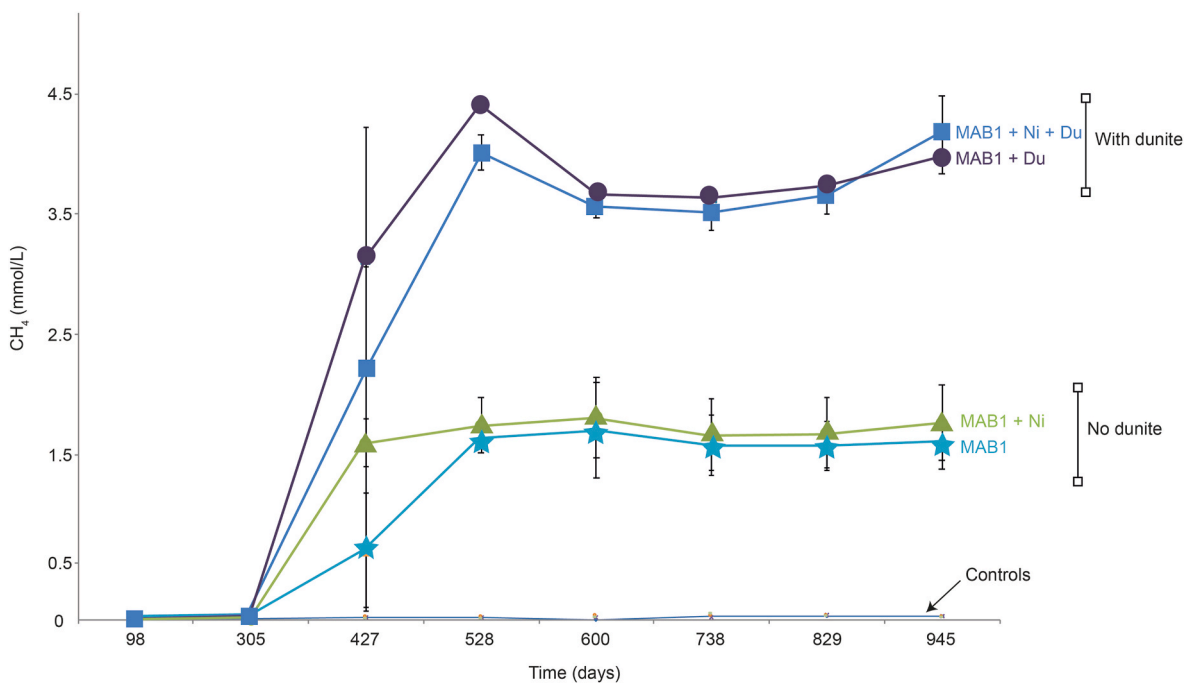
Fig. 3. Average (of three replicates) accumulation of methane (CH_4, mM) over time in the incubation bottles and abiotic controls. Open symbols represent experiments with added dunite, filled symbols without added dunite. Dashed lines represent control samples.

Table 3

Mean concentration (μg L-1) of major elements and acetate in controls and inoculated experiments. <DL = below detection limit. Si = silicon (DL = 3.89 μg L-1), Mg = magnesium (DL = 0.08 μg L-1), Ni = nickel (DL = 10.3 μg L-1), Fe = iron (DL = 2.96 μg L-1), Zn = zinc (DL = 3.81 μg L-1).

Experiment	Si	Mg	Ni	Fe	Zn	Acetate (g/L)
Non-dunite controls	45.26 ± 4.30	7.66 ± 4.78	<DL	<DL	<DL	0.27 ± 0.12
Dunite controls	54.02 ± 5.91	69.58 ± 30.39	0.96 ± 0.67	3.46 ± 4.24	182.29 ± 14.87	0.34 ± 0.08
Non-dunite inoculated	32.92 ± 13.72	5.56 ± 3.61	<DL	<DL	<DL	0.03 ± 0.01
Dunite inoculated	56.85 ± 5.65	23.75 ± 3.97	0.13 ± 0.11	<DL	201.72 ± 22.33	0.26 ± 0.11
Initial conc	<DL	<DL	50	2000	<DL	0.42

SEM analyses) after termination of the experiment and used for extraction of DNA and qPCR analyses of methanogens. In all samples from the non-inoculated controls, methanogenic gene abundance was below detection limit ($<10^3$ copies mL^{-1} growth medium), whereas all inoculated samples (except 2c) clearly showed presence of the methanogen (Table 4). Melt point analyses illustrated a single melting point at expected temperature for all amplicons generated from the inoculated samples, confirming a specific PCR product. With one exception (2b), the qPCR results showed slightly higher gene copy abundance (gene copy/mL) in the dunite-free inoculates than in those containing dunite (Table 4).

As mentioned above, microscopy analysis showed indications of bacterial contamination and DNA was consequently also used for PCR analyses targeting bacteria. In this way bacterial contamination were found in the biological samples without added dunite (MAB1 + Ni and MAB1). The obtained PCR products were sequenced (Sanger) and the results illustrated that the amplified bacterial sequence affiliated to the Firmicutes phylum and were closely related (98 %) to *Limnochorda pilosa* strain HC45^T (GenBank/EMBL/DDBJ accession number: AB992259).

3.6. Statistical analyses

One-way MANOVA showed that all experiments performed under the same conditions were similar, with $P > 0.05$, regarding CH$_4$ production and H$_2$ and CO levels (Table 5). MANOVA between biotic and abiotic samples incubated under the same conditions showed that all sets of pairs were significantly different ($P < 0.05$) (Table 5).

PCA analysis using Pearson correlation (chosen for direct, linear trends between variables) coefficient revealed that abiotic controls clustered together, while the biotic experiments were distributed into two clusters: one comprised of experiments performed without dunite, with or without Ni (samples 8 and 4), and one comprised of experiments performed with dunite, with or without Ni (samples 6, 2, and 1), with the exception of one replicate of batch 1 (MAB1 incubated with Ni and dunite) (Fig. 5). The PCA thus suggested a significant effect of dunite in

Table 4

Total methanogenic 16S rRNA gene abundance per mL of growth medium (average of three replicates) measured after termination of the experiments. Standard deviation represents the variance for three biological replicates. For treatment abbreviations, see Table 1.

Experiment	Av. log. gen.ab.	Stdev
MAB1 + Ni + Du	4.01E+06	3.58E+06
MAB1 + Du	1.27E+05	1.78E+04
MAB1 + Ni - Du	3.94E+07	1.22E+07
MAB1	7.49E+07	4.56E+07
Control + Ni + Du	No signal	No signal
Control + Ni + Du	No signal	No signal
Control + Du	No signal	No signal
Control	No signal	No signal
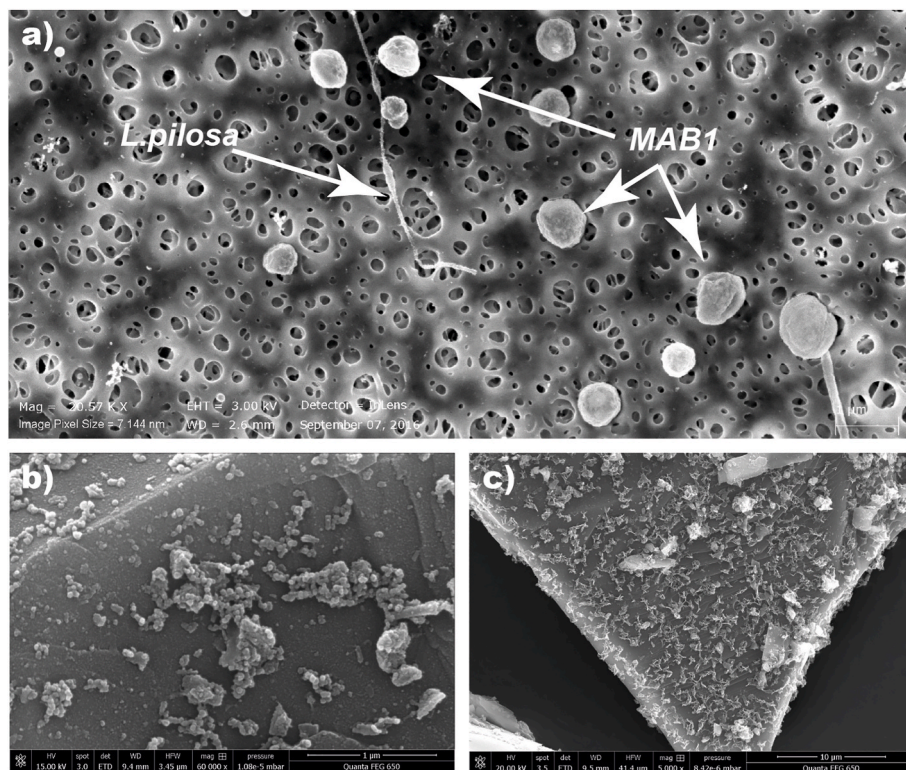
Fig. 4. Scanning electron microscope (SEM) images of dunite grain surface at the end of the experiment showing a) presence of filaments and irregular cocci, b) small spherical structures of approximately 0.1 μm in size, and c) alteration minerals covering the dunite grain surfaces.

Table 5
P-values obtained in MANOVA (Wilks' lambda test) for each replicate of the same batch of experiments and between abiotic and biotic experiments performed under the same conditions. Bold values indicate significance (P < 0.05).

Conditions	Abiotic experiments	*P*-value	Biotic experiments	*P*-value	Abiotic versus biotic experiments	*P*-value
With Ni and with dunite	3	0.364	1	0.073	3 vs 1	**<0,0001**
Without Ni and with dunite	9	0.983	2 + 6	0.916	9 vs 2 + 6	**<0,0001**
With Ni and without dunite	5	0.533	4	0.788	5 vs 4	**<0,0001**
Without Ni and without dunite	10	0.102	8	0.210	10 vs 8	**<0,0001**

the biotic experiments, while the presence or absence of Ni did not seem to be the main parameter impacting CH_4 production and CO and H_2 consumption (Fig. 5).

One-way ANOVA analysis, comparing biotic CH_4 production in the presence of dunite with or without Ni (batch 1 against batch 2 + 6) resulted in a *P*-value close to zero (0.0004) (Table 6), i.e., presence/absence of Ni significantly affected CH_4 production in the presence of dunite. A *P*-value close to zero was also found for CH_4 production in the presence of Ni with or without dunite (batch 1 against 4), suggesting that Ni affected CH_4 production. Moreover, CH_4 production in the presence of Ni and dunite (batch 1) was significantly different (*P* = 0.0004) from CH_4 production without Ni and without dunite (batch 8). Contrary to these significant trends, CH_4 production in the absence of dunite with or without Ni (batch 4 against 8) did not differ (*P* > 0.05) from CH_4 production in the absence of Ni with or without dunite (batch 2 against 8).

4. Discussion

Hydrous alteration of ultramafic rocks, such as dunite, can lead to the reduction of water to H_2 as Fe(II) in dunite is oxidized to Fe(III) in secondary serpentine or magnetite minerals. Formation of serpentine minerals is known to release H_2, serving as an indicator of mineral

Table 6
P-values obtained in ANOVA for methane (CH_4) production in biotic experiments. Bold values indicate significance (P < 0.05).

Condition	Experiment	*P* value
With Ni and with dunite	1	0.0004
Without Ni and with dunite	2 + 6	
With Ni and with dunite	1	0.0004
With Ni and without dunite	4	
With Ni and with dunite	1	0.0004
Without Ni and without dunite	8	
Without Ni and with dunite	2 + 6	0.0004
With Ni and without dunite	4	
Without Ni and with dunite	2 + 6	0.201
Without Ni and without dunite	8	
With Ni and without dunite	4	0.292
Without Ni and without dunite	8	

alteration processes. This serpentinization reaction, and the associated H_2 production, is most significant around 300 °C and is extremely slow at temperatures below 100 °C [23]. Our experiments confirm that abiotic H_2 formation is very low under low-temperature conditions (Fig. 1). Abiotic H_2 production was minimal, consistent with previous reports on low-temperature olivine and dunite alteration [12]. Still, H_2
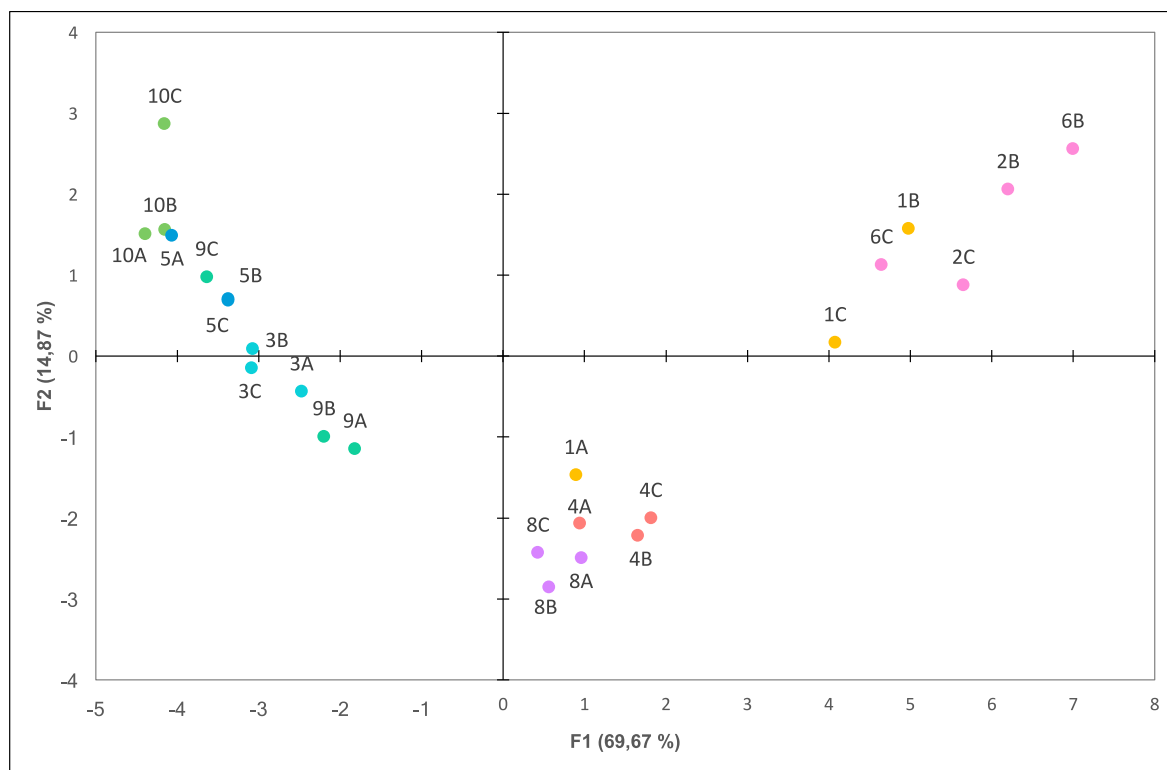

Fig. 5. Principal component analysis plot of samples used in this study. The two main axes explain 84.54 % of the variance in CH_4 production and CO and H_2 levels. Points 3, 5, 9, and 10 represent the abiotic controls (3: with Ni and with dunite; 5: with Ni and without dunite; 9: without Ni and with dunite; 10: without Ni and without dunite), while points 1, 2, 4, 6, and 8 represent the experiments inoculated with MAB1 (1: with Ni and with dunite; 2, 6: without Ni and with dunite; 4 with Ni and without dunite; 8: without Ni and without dunite).

production reached levels previously shown to support growth of the investigated *Methanocullues* strain [12]. However, even though the results showed methane production, the H_2 release was apparently not sufficient for sustained methanogenic growth. Interestingly, H_2 production increased in the presence of methanogens (Fig. 1). The H_2 levels in the inoculated dunite bottles were higher compared to abiotic controls, where no significant difference in H_2 levels was observed with or without added dunite. These results suggest that the methanogenic activity somehow increased H_2 production from dunite, while some H_2 might also have been released from the decomposition of dead cells [24]. Abiotic degradation of organic litter (plant material) in the absence of O_2 and at temperatures similar to those used in our study have been shown to produce H_2 at a rate of approximately 0.2 nmol m^{-2} s^{-1} [24]. Another source of H_2 except from the dunite or degradation of cells, could have been by the breakdown of acetate. Abiotic acetate oxidation is not favorable under our experimental conditions, even with a strong catalyst, however the process can be biologically catalyzed, also under methanogenic conditions [25]. Oxidation of acetate is highly unfavorable energetically ($\Delta G0' = +94.9$ kJ/mol) but can proceed if H_2 is removed by a hydrogenotrophic consuming methanogens, like MAB1 ($\Delta G0' = -135.6$ kJ/mol) [26,27]. The oxidation of acetate could have been performed by a contaminating bacterium. Microscopic analysis revealed the presence of the irregular coccoid-shaped methanogen but also a filamentous bacterium, indicating bacterial contamination, also supported by DNA analysis. Sequence analysis illustrated that the contaminant, likely present in low abundance in the methanogenic inoculum, was closely related to *Limnochorda pilosa*, a facultative anaerobe known to form filaments and membrane vesicles, as observed in SEM images. This bacterium primarily ferments carbohydrates, but its weak growth on acetate may explain its presence in the experiment [22]. Inoculated bottles without dunite showed comparably lower acetate levels, suggesting acetate utilization. In contrast, bottles with dunite had higher acetate levels, indicating that the bacterium did not thrive in the dunite-altered environment, where higher H_2 levels also were detected (Table 3). Partial pressures of H_2 needs to be approximately 4 μM or lower for acetate oxidation [24,25] and the pH$_2$ values in the dunite bottles did not fall below 0.5 mM (Table 2), which would prevent any acetate oxidation.

Stoichiometrically, approximately equal amount of CH_4 can be produced per acetate consumed [28], which in our case corresponded to approximately 1 mmol/L. This is close to the amounts of CH_4 observed in the inoculated bottles without added dunite. However, CH_4 production was higher in the dunite containing bottles, why acetate could not have been the only source of CH_4 formation in these bottles, specifically considering that most of the acetate was still not converted in these cultures. Thus, the higher levels of H_2 in the inoculated bottles with dunite suggest that CH_4 was still produced mainly from dunite-derived H_2.

The initial growth medium and gas phase were strongly reduced (Eh < −110 mV), which may convert CO_2 to CO according to the standard reduction potential of −104 mV in water following reaction 2 [29]. This could explain the presence of CO in the bottles.

$$CO_{2(g)} + 2e\text{-} + 2H^+ = CO_{(g)} + H_2O \quad (2)$$

$$(2n + 1)H_2 + nCO \rightarrow C_nH_{(2n+2)} + nH_2O \quad (3)$$
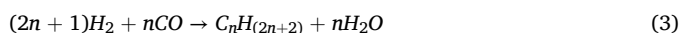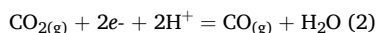
Under certain circumstances, CO_2 or CO can be catalytically reduced to CH_4 through the so-called Fischer-Tropsch reaction (FT, reaction 3) or the Fischer-Tropsch Type reaction (FTT, reaction 1, same as reaction for microbial methanogenesis). However, these reactions are most efficient at temperatures above 200 °C [30,31]. In the set-up used here, with an experimental temperature of 37 °C, formation of CH_4 through such process would be a very slow process, even in the presence of catalytic sites such as chromium spinels on the dunite surface. Also, the CH_4 production in the inoculated controls were higher as compared to the inoculated bottles, showing that CH_4 could not only have been produced

by such abiotic process.

Some methanogens can use CO as an energy source, though growth is slow and may be incompatible with methanogenesis due to CO toxicity or redox imbalances [32]. However, at CO concentrations below 10 %, some methanogens have been shown to utilize CO as the sole energy source after a 500-h lag phase, provided that sufficient H_2 was available [33]. Several methanogenic strains have been shown to be able to utilize CO, but the research on methanogenic CO utilization is still scarce and no information on *M. bourgensis* and CO is available. Thus, it is only possible to speculate as to whether MAB1 can use CO or not.

Methane production was sustained in all but one inoculated bottle (exp. 2A) for nearly three years without external nutrient or energy input. CH_4 production was faster and higher in bottles with dunite, suggesting sufficient H_2 production from dunite to support methanogenic growth. Also, previous studies have shown that the levels of H_2 measured here is sufficient for the growth of MAB1 [12]. However, CH_4 production in bottles without dunite indicates an additional H_2 source, as discussed above. Despite sufficient H_2 release from dunite, CH_4 production ceased after 528 days, likely due to trace element toxicity from dunite, as heavy metals like Zn can inhibit methanogen growth at concentrations observed in the experiments [34].

Quantification of the methanogen, using qPCR at the end of the experiment (day 829) showed a higher abundance in cultures without dunite (batches 4 and 8) compared to inoculates with added dunite (batches 2,6 and 1). An explanation to these somewhat contradictory results, considering the higher CH_4 production in the dunite supplemented bottles, could be that dunite provide an initial supply of H_2, leading to a methanogenic growth and CH_4 production, but after some time, the toxicity of the dunite becomes too high and the methanogenic growth was inhibited. This inhibition effect was further supported by the inability of the methanogenic cells to respond to externally added H_2 while on the contrary a significant increase of CH_4 was seen for the non-dunite supplemented bottles. Approximately 30 % of the added H_2 was converted to CH_4. The amount of Ni in the growth medium had minimal impact on CH_4 levels, causing only a slight delay in CH_4 formation. A previous study showed that H_2 uptake was slightly more efficient with Ni, but Ni was not essential for growth [12]. In this study, H_2 levels decreased slightly faster in Ni-containing bottles early on, but after one year, the differences became insignificant, indicating that only a small amount of Ni is needed and that Ni concentration was not a limiting factor.

5. Conclusions

Cultures supplemented with dunite produced more CH_4 compared to those without, indicating a positive effect of dunite addition, likely because formation of H_2 due to abiotic and/or biologic alteration of dunite. Methane production began slowly after approximately 300 days, aligning with a decrease in hydrogen levels. The H_2 levels measured were within the range supporting the growth of *Methanoculleus bourgensis*, as shown in prior studies. Some CH_4 was likely produced with indirect assistance from a bacterial contaminant closely related to *L. pilosa*, through acetate oxidation to H_2 and CO_2, which the methanogen later utilized. However, this acetate-driven process was only observed in non-dunite cultures and could not account for the observed CH_4 yields.

Methane production continued for about 528 days before ceasing, possibly due to inhibitory levels of trace metals released during dunite alteration, such as zinc, which likely inhibited methanogen growth. Addition of external energy source (H_2) to investigate methanogenic survival supported the inhibitory effect of dunite as only cultures without dunite showed responded with methane production. Noteworthy was that the methanogen survived and showed activity for over 800 days.

In summary, the results suggest that low-temperature alteration of ultramafic rocks like dunite can support methanogen growth. However,

this growth is limited by the slow rate of H_2 production and the accumulation of toxic trace elements.

CRediT authorship contribution statement

A. Neubeck: Writing – review & editing, Writing – original draft, Visualization, Validation, Supervision, Resources, Project administration, Methodology, Investigation, Funding acquisition, Formal analysis, Data curation, Conceptualization. **N. Callac:** Writing – review & editing, Validation, Methodology, Investigation, Formal analysis, Data curation, Conceptualization. **S. Isaksson:** Writing – review & editing, Validation, Methodology, Formal analysis, Data curation. **A. Schnürer:** Writing – review & editing, Validation, Supervision, Resources, Methodology, Investigation, Data curation, Conceptualization.

Declaration of competing interest

The authors declare that they have no known competing financial interests or personal relationships that could have appeared to influence the work reported in this paper.

Acknowledgements

Data availability

All data is presented in the manuscript.

References

[1] K. Raymann, C. Brochier-Armanet, S. Gribaldo, The two-domain tree of life is linked to a new root for the Archaea, Proc. Natl. Acad. Sci. USA 112 (21) (2015) 6670–6675, https://doi.org/10.1073/pnas.1420858112.

[2] C. Huber, G. Wächtershäuser, Activated acetic acid by carbon fixation on (Fe,Ni)S under primordial conditions, Science 276 (5310) (Apr. 1997) 245–247, https://doi.org/10.1126/science.276.5310.245.

[3] J.B. Moody, Serpentinization: a review, Lithos 9 (2) (Apr. 1976) 125–138, https://doi.org/10.1016/0024-4937(76)90030-X.

[4] W.B. Whitman, T.L. Bowen, D.R. Boone, The methanogenic bacteria, in: M. Dworkin, S. Falkow, E. Rosenberg, K.-H. Schleifer, E. Stackebrandt (Eds.), The Prokaryotes: Volume 3: Archaea. Bacteria: Firmicutes, Actinomycetes, Springer, New York, NY, 2006, pp. 165–207, https://doi.org/10.1007/0-387-30743-5_9.

[5] R.-S. Taubner, et al., Biological methane production under putative Enceladus-like conditions, Nat. Commun. 9 (Feb) (2018), https://doi.org/10.1038/s41467-018-02876-y.

[6] R.K. Thauer, A.-K. Kaster, H. Seedorf, W. Buckel, R. Hedderich, Methanogenic archaea: ecologically relevant differences in energy conservation, Nat. Rev. Microbiol. 6 (8) (Aug. 2008) 579–591, https://doi.org/10.1038/nrmicro1931.

[7] D. Payne, R.L. Spietz, E.S. Boyd, Reductive dissolution of pyrite by methanogenic archaea, ISME J. 15 (12) (Dec. 2021) 3498–3507, https://doi.org/10.1038/s41396-021-01028-3.

[8] C. Yamada, S. Kato, S. Kimura, M. Ishii, Y. Igarashi, Reduction of Fe(III) oxides by phylogenetically and physiologically diverse thermophilic methanogens, FEMS (Fed. Eur. Microbiol. Soc.) Microbiol. Ecol. 89 (3) (Sep. 2014) 637–645, https://doi.org/10.1111/1574-6941.12365.

[9] H. Jung, H. Yu, C. Lee, Direct interspecies electron transfer enables anaerobic oxidation of sulfide to elemental sulfur coupled with CO2-reducing methanogenesis, iScience 26 (9) (Sep. 2023) 107504, https://doi.org/10.1016/j.isci.2023.107504.

[10] S. Ragsdale, The eastern and western branches of the wood/ljungdahl pathway, Biofactors 9 (1997) 1–9.

[11] R.K. Thauer, A.-K. Kaster, M. Goenrich, M. Schick, T. Hiromoto, S. Shima, Hydrogenases from methanogenic archaea, nickel, a novel cofactor, and H2

[12] storage, Annu. Rev. Biochem. 79 (2010) 507–536, https://doi.org/10.1146/annurev.biochem.030508.152103.

[12] A. Neubeck, S. Sjöberg, A. Price, N. Callac, A. Schnürer, Effect of nickel levels on hydrogen partial pressure and methane production in methanogens, PLoS One 11 (12) (Dec. 2016) e0168357, https://doi.org/10.1371/journal.pone.0168357.

[13] M. Westerholm, S. Roos, A. Schnürer, Syntrophaceticus schinkii gen. nov., sp. nov., an anaerobic, syntrophic acetate-oxidizing bacterium isolated from a mesophilic anaerobic filter, FEMS (Fed. Eur. Microbiol. Soc.) Microbiol. Lett. 309 (1) (Aug. 2010) 100–104, https://doi.org/10.1111/j.1574-6968.2010.02023.x.

[14] P. Scherer, H. Lippert, G. Wolff, Composition of the major elements and trace elements of 10 methanogenic bacteria determined by inductively coupled plasma emission spectrometry, Biol. Trace Elem. Res. 5 (3) (Jun. 1983) 149–163, https://doi.org/10.1007/BF02916619.

[15] R.K. Watt, P.W. Ludden, Nickel-binding proteins, CMLS Cell. Mol. Life Sci. 56 (7) (Nov. 1999) 604–625, https://doi.org/10.1007/s000180050456.

[16] S. Ehinger, J. Seifert, A. Kassahun, L. Schmalz, N. Hoth, M. Schlömann, Predominance of methanolobus spp. and Methanoculleus spp. in the archaeal communities of saline gas field formation fluids, Geomicrobiol. J. 26 (Jun. 2009) 326–338, https://doi.org/10.1080/01490450902754441.

[17] J.A. Mikucki, Y. Liu, M. Delwiche, F.S. Colwell, D.R. Boone, Isolation of a methanogen from deep marine sediments that contain methane hydrates, and description of Methanoculleus submarinus sp. nov, Appl. Environ. Microbiol. 69 (6) (Jun. 2003) 3311–3316, https://doi.org/10.1128/AEM.69.6.3311-3316.2003.

[18] M. Westerholm, L. Levén, A. Schnürer, Bioaugmentation of syntrophic acetate-oxidizing culture in biogas reactors exposed to increasing levels of ammonia, Appl. Environ. Microbiol. 78 (21) (Nov. 2012) 7619, https://doi.org/10.1128/AEM.01637-12.

[19] N.E. Odongo, et al., Long-term effects of feeding monensin on methane production in lactating dairy cows, J. Dairy Sci. 90 (4) (Apr. 2007) 1781–1788, https://doi.org/10.3168/jds.2006-708.

[20] D.J. Lane, B. Pace, G.J. Olsen, D.A. Stahl, M.L. Sogin, N.R. Pace, Rapid determination of 16S ribosomal RNA sequences for phylogenetic analyses - pmc, Proc. Natl. Acad. Sci. USA 82 (20) (1985) 6955–6959.

[21] K.-O. Habermehl (Ed.), Rapid Methods and Automation in Microbiology and Immunology, Springer, Berlin, Heidelberg, 1985, https://doi.org/10.1007/978-3-642-69943-6.

[22] M. Watanabe, H. Kojima, M. Fukui, Limnochorda pilosa gen. nov., sp. nov., a moderately thermophilic, facultatively anaerobic, pleomorphic bacterium and proposal of Limnochordaceae fam. nov., Limnochordales ord. nov. and Limnochordia classis nov. in the phylum Firmicutes, Int. J. Syst. Evol. Microbiol. 65 (Pt_8) (2015) 2378–2384, https://doi.org/10.1099/ijs.0.000267.

[23] A. Neubeck, et al., Olivine alteration and H2 production in carbonate-rich, low temperature aqueous environments, Planet. Space Sci. 96 (2014) 51–61, https://doi.org/10.1016/j.pss.2014.02.014.

[24] H. Lee, T. Rahn, H.L. Throop, A novel source of atmospheric H2: abiotic degradation of organic material, Biogeosciences 9 (11) (2012) 4411–4419, https://doi.org/10.5194/bg-9-4411-2012.

[25] S. Hattori, Syntrophic acetate-oxidizing microbes in methanogenic environments, Microb. Environ. 23 (2) (2008) 118–127, https://doi.org/10.1264/jsme2.23.118.

[26] M.J. Lee, S.H. Zinder, Hydrogen partial pressures in a thermophilic acetate-oxidizing methanogenic coculture, Appl. Environ. Microbiol. 54 (6) (Jun. 1988) 1457–1461.

[27] S.H. Zinder, M. Koch, Non-aceticlastic methanogenesis from acetate: acetate oxidation by a thermophilic syntrophic coculture, Arch. Microbiol. 138 (3) (Jul. 1984) 263–272, https://doi.org/10.1007/BF00402133.

[28] H. Weber, K.D. Kulbe, H. Chmiel, W. Trösch, Microbial acetate conversion to methane: kinetics, yields and pathways in a two-step digestion process, Appl. Microbiol. Biotechnol. 19 (4) (Apr. 1984) 224–228, https://doi.org/10.1007/BF00251840.

[29] S.G. Bratsch, Standard electrode potentials and temperature coefficients in water at 298.15 K, J. Phys. Chem. Ref. Data 18 (Jan. 1989) 1–21, https://doi.org/10.1063/1.555839.

[30] D.G. Capone, D.D. Reese, R.P. Kiene, Effects of metals on methanogenesis, sulfate reduction, carbon dioxide evolution, and microbial biomass in anoxic salt marsh sediments, Appl. Environ. Microbiol. 45 (5) (May 1983) 1586–1591, https://doi.org/10.1128/aem.45.5.1586-1591, 1983.

[31] E.J. Kroeker, D.D. Schulte, A.B. Sparling, H.M. Lapp, Anaerobic treatment process stability, Journal (Water Pollution Control Federation) 51 (4) (1979) 718–727.

[32] C. Schöne, M. Rother, Methanogenesis from carbon monoxide, in: A.J.M. Stams, D. Z. Sousa (Eds.), Biogenesis of Hydrocarbons, Springer International Publishing, Cham, 2019, pp. 123–151, https://doi.org/10.1007/978-3-319-78108-2_4.

[33] M. Diender, A.J.M. Stams, D.Z. Sousa, Pathways and bioenergetics of anaerobic carbon monoxide fermentation, Front. Microbiol. 6 (Nov) (2015), https://doi.org/10.3389/fmicb.2015.01275.

[34] M. Kumar, et al., Effect of varying zinc concentrations on the biomethane potential of sewage sludge, Water 15 (4) (2023), https://doi.org/10.3390/w15040729.